ELSEVIER

Polymer 41 (2000) 1607–1614

polymer

Hydrodynamic dimensions of heteroarm star copolymers by size exclusion chromatography

C. Tsitsilianis[a,b,*], D. Voulgaris[a,b]

[a]*Department of Chemical Engineering, University of Patras, 26500 Patras, Greece*
[b]*Institute of Chemical Engineering and High Temperature Chemical Processes, ICE/HT-FORTH, P.O. Box 1414, 26500 Patras, Greece*

Received 1 January 1999; received in revised form 14 April 1999; accepted 21 April 1999

Abstract

Heteroarm star copolymers, i.e. star-shaped polymers bearing A and B pure arms (type A_nB_n) were synthesized by anionic polymerization and their hydrodynamic properties in a common good solvent were investigated by means of size exclusion chromatography. The proposed method allows the study of the evolution of the hydrodynamic dimensions of the heteroarm star copolymers as the second generation of the arms is growing from the cores. Different growth rates of the A_nB_n star size were observed which are influenced by three factors: the number of arms, the ratio of the size of the chemically different arms and the interactions between the unlike segments. The last factor is affected significantly by the selectivity of the solvent. © 1999 Elsevier Science Ltd. All rights reserved.

Keywords: Heteroarm star copolymers; Size exclusion chromatography; Hydronamic dimensions

1. Introduction

Star-shaped block copolymers exhibiting novel architectures have been synthesized by "living" polymerization techniques and the study of their properties in solution as well as in the bulk, has received much attention in the recent years [1–5].

Our efforts have been focused on the heteroarm star copolymers which are star-shaped macromolecules constituted from a central poly(DVB) core bearing equal number of A and B arms (type A_nB_n) [1,6–8].

Their synthesis is performed via an anionic copolymerization method comprising three sequential steps [1]. In the first two steps a star-shaped polymer (A_n) is formed by reacting a living linear precursor (arms A) with a bis-unsaturated monomer (e.g. divinylbenzene). The resulting star polymer is still "living", bearing within its core a number of "living' sites equal to the number of the arms incorporated in the star molecule. These sites are able to initiate the polymerization of another suitable monomer. In the third step a new set of arms is growing from the core yielding the heteroarm star copolymer (A_nB_n).

Recently the solution properties of the heteroarm star copolymers, in common good solvents as well as in selective solvents have been reported [7,9–15]. As have been shown, the architecture of the macromolecule plays an important role on the micellar properties of block copolymers. Critical micelle concentrations, aggregation numbers, hydrodynamic dimensions and microdomain sizes of micelles afforded by star-shaped A_nB_n copolymers differ remarkably from those afforded by the linear AB diblock copolymers.

The aim of the present article is firstly to report on the solution properties of the A_nB_n heteroarm star copolymers in a common good solvent for the different arms and secondly to show how one can use the size exclusion chromatography to obtain information concerning the hydrodynamic dimensions of these macromolecules with the specific topology. Especially we look how the molecular characteristics of the star copolymers such as the different arms length ratio, the number of arms and the interactions between the unlike segments influence the hydrodynamic size of the A_nB_n star copolymer.

2. Experimental part

2.1. Synthetic procedure

All the heteroarm star copolymers were synthesized by anionic polymerization under argon atmosphere using THF as solvent. The procedure used is a three step sequential "living" copolymerization method which allows the

* Corresponding author. Department of Chemical Engineering, University of Patras, Patras, Greece.

PII: S0032-3861(99)00315-8

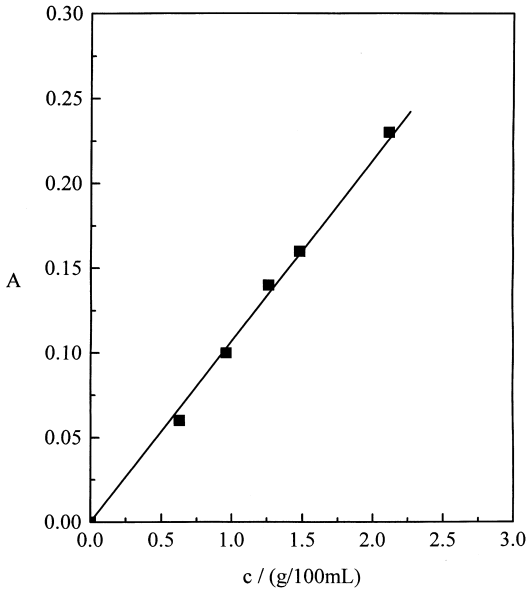

Fig. 1. Absorbance at 1730 cm^{-1} as a function of the concentration of poly(ethyl methacrylate).

preparation, from the same reaction, of a series of star copolymers differing only in the length of the second generation of arms (PEMA, PtBA and P2VP).

In the first step the PS arms were synthesized, using sec-butyl lithium as initiator, at −40°C in the presence of LiCl. In the second step a small amount of DVB was polymerized by the living polystyril lithium chains, yielding star-shaped polystyrene (PS_n). These star polymers are still "living", bearing a number of active sites equal to the number of their arms. In the third step these active sites are used to polymerize another monomer such as ethylmethacrylate (EMA), tert-butyl acrylate (tBA) and 2-vinylpyridine (2VP). The polymerization of EMA and tBA was carried out at −60°C and for 2VP at −78°C. In this step parts of the reaction mixture were withdrawn following every time the addition of another amount of monomer. The active sites were deactivated by the addition of degassed methanol. Moreover, in every synthesis an appropriate amount of solution was sampled out after the completion of styrene and DVB polymerization, for the purpose of characterization. The PS_nPEMA_n and PS_nPtBA_n copolymers were precipitated in a methanol/water mixture (80/20, v/v) and the PS_nP2VP_n copolymers in cold heptane.

2.2. Characterization

The M_w of the PS arms was obtained by SEC using PS standards. The M_w of the PS_n was determined by multiangle laser light scattering in THF at 25°C using the model SEM RD spectrogoniometer (Sematech, France) equipped with a He–Ne laser (633 nm). The weight average functionality n of the PS_n was calculated by the equation

$$n = \frac{M_w(PS_n)}{M_w(PS_{arm}) + m_o[DVB]/[LE]} \quad (1)$$

where m_o is the molecular weight of divinyl benzene and [DVB]/[LE] is the divinylbenzene per living ends mole ratio.

The weight content, W, of PEMA and PtBA in PS_nPEMA_n and PS_nPtBA_n copolymers respectively was determined by IR spectroscopy which was carried out on a Perkin–Elmer 16PC apparatus. The polymer solutions in CCl_4 were recorded with a NaCl cell. The carbonyl group of PEMA and PtBA gives a very strong and narrow absorption in the infrared region at 1730 cm^{-1}. Subsequently FTIR spectroscopy can be used to determine the PEMA and PtBA content of the copolymers. The procedure consisted in calibrating a NaCl cell with PEMA and PtBA homopolymer solutions in CCl_4 and determining the absorbance A_{1730} of a solution of the copolymer of known concentration in the same cell. The plot of absorbance at 1730 cm^{-1} as a function of the

Table 1
Characterization data of PS_nPEMA_n copolymers

Sample[a]	M_w (PS_{arm}) ($\times 10^{-4}$ g/mol)	M_w (PS_n) ($\times 10^{-4}$ g/mol)	n	W_{PEMA} (%)	M_w ($PEMA_{arm}$) ($\times 10^{-4}$ g/mol)
$PS_4PEMA_4$26	2.6	11.7	4.4	26.0	0.93
$PS_4PEMA_4$50	2.6	11.7	4.4	50.45	2.70
$PS_4PEMA_4$58	2.6	11.7	4.4	57.9	3.66
$PS_4PEMA_4$62	2.6	11.7	4.4	62.3	4.39
$PS_4PEMA_4$67	2.6	11.7	4.4	67.3	5.46
$PS_6PEMA_6$19	3.4	24.1	6.3	18.95	0.89
$PS_6PEMA_6$37	3.4	24.1	6.3	36.5	2.20
$PS_6PEMA_6$52	3.4	24.1	6.3	52.3	4.19
$PS_6PEMA_6$57	3.4	24.1	6.3	56.7	5.02
$PS_6PEMA_6$61	3.4	24.1	6.3	60.9	5.95
$PS_9PEMA_9$19	2.0	20.0	9.0	18.5	0.50
$PS_9PEMA_9$36	2.0	20.0	9.0	36.4	1.27
$PS_9PEMA_9$51	2.0	20.0	9.0	50.9	2.30
$PS_9PEMA_9$59	2.0	20.0	9.0	58.9	3.19
$PS_9PEMA_9$63	2.0	20.0	9.0	62.5	3.70

[a] A_nB_nW: A and B are the kind of arms, n stands for the weight average functionality and W the weight content of PEMA in the copolymers.

Table 2
Characterization data of PS_nPtBA_n copolymers

Sample[a]	M_w (PS_{arm}) ($\times 10^{-4}$ g/mol)	M_w (PS_n) ($\times 10^{-4}$ g/mol)	n	W_{PtBA} (%)	M_w ($PtBA_{arm}$) ($\times 10^{-4}$ g/mol)
$PS_4PtBA_4$26	2.8	13.8	4.7	26.0	1.03
$PS_4PtBA_4$40	2.8	13.8	4.7	39.9	1.95
$PS_4PtBA_4$48	2.8	13.8	4.7	47.7	2.68
$PS_4PtBA_4$53	2.8	13.8	4.7	53.3	3.35
$PS_4PtBA_4$56	2.8	13.8	4.7	56.4	3.82

[a] A_nB_nW: the same as in Table 1, where W stands for the weight content of PtBA in the copolymers.

concentration of PEMA or PtBA is a straight line ($r = 0.999$) (Fig. 1), as expected from the Beer–Lambert law. Thus W was calculated from the equation

$$W = \frac{A_{1730}}{bc} \tag{2}$$

where b is the slope of calibration curve and c the concentration in g/100 cm^3.

The weight content of P2VP in PS_nP2VP_n copolymers was determined by ^1H NMR from the integrated peak intensities corresponding to the *a* proton in the aromatic pyridine group (8.0–8.3 ppm) compared to the rest of the aromatic protons (6.3–7.4 ppm). The ^1H NMR spectra of PS_nP2VP_n diluted in $CDCl_3$ were recorded on a Bruker AMX-400 (400 MHz) spectrometer.

Provided that the PS and PEMA arms are equal, the molecular weight of the PEMA arms can be calculated by the formula

$$M_w(\mathrm{PEMA_{arm}}) = \frac{M_w(\mathrm{PS}_n)W_{\mathrm{PEMA}}}{n(1 - W_{\mathrm{PEMA}})}. \tag{3}$$

In the case of PS_nPtBA_n and PS_nP2VP_n copolymers PEMA in Eq. (3) is replaced by PtBA and P2VP respectively. The molecular characteristics of heteroarm star copolymers are given in Tables 1–3.

2.3. Size exclusion chromatography (SEC)

SEC was carried out using a model 201 apparatus equipped with a model 401 differential refractometer as detector (Water Associates). A set of three μ-Styragel columns (10^3, 10^4 and 10^5 Å) was used and the calibration curve was obtained by PS standards. The mobile phase was tetrahydrofuran (analytical grade) and the flow rate was 1 cm^3 min^{-1}. In the case of PS_nP2VP_n copolymers SEC was performed with a mixture of tetrahydrofuran and triethylamine (THF/Et_3N, 99/1, v/v) to prevent adsorption of P2VP in the columns.

3. Results and discussion

SEC is a chromatographic technique for which the separation mechanism relies on the size of the macromolecules under analysis. In the case where interactions between the macromolecule and the sorbent are negligible the retention volume V_R of a macromolecule is related to its hydrodynamic dimensions.

According to the universal calibration concept the chromatographic data can be evaluated through the relationship

$$\log V_h = A' - B'V_R \tag{4}$$

where V_h is the hydrodynamic volume of the macromolecules and A', B' are constants related every time to the chromatographic system. For the heteroarm star copolymer, A_nB_n, and the star precursor it originated from, A_n, Eq. (4) can be written as

$$\log V_h^{**} = A' - B'V_R^{**} \tag{5}$$

and

$$\log V_h^{*} = A' - B'V_R^{*} \tag{6}$$

where superscripts $*$ and $**$ denote A_n and A_nB_n star respectively. Subtracting Eqs. (5) and (6) we obtain

$$\log \frac{V_h^{**}}{V_h^{*}} = B'\Delta V_R \tag{7}$$

where $\Delta V_R = V_R^{*} - V_R^{**}$. Therefore the difference between the retention volumes of the A_nB_n star and its A_n star precursor, reflects their hydrodynamic volume ratio (i.e.

Table 3
Characterization data of PS_nP2VP_n copolymers

Sample[a]	M_w (PS_{arm}) ($\times 10^{-4}$ g/mol)	M_w (PS_n) ($\times 10^{-4}$ g/mol)	n	W_{P2VP} (%)	M_w ($P2VP_{arm}$) ($\times 10^{-4}$ g/mol)
$PS_6P2VP_6$24	2.3	15.6	6.1	24	0.81
$PS_6P2VP_6$44	2.0	15.4	6.9	44	1.75
$PS_6P2VP_6$60	2.0	15.4	6.9	60	4.33
$PS_6P2VP_6$66	2.0	15.4	6.9	66	4.33

[a] A_nB_nW: the same as in Table 1, where W stands for the weight content of P2VP in the copolymers.

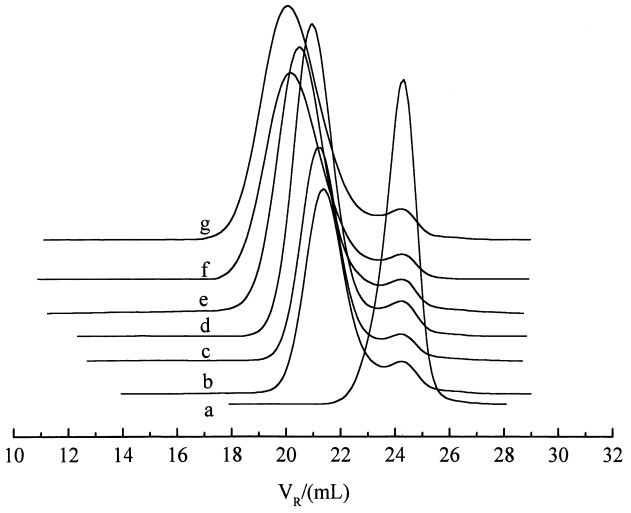

Fig. 2. GPC chromatograms of (a) lPS, (b) PS_n and (c)–(g) PS_9PEMA_9 copolymers with increasing W_{PEMA}.

normalized hydrodynamic volume of the heteroarm star) and is used to monitor the evolution of the hydrodynamic dimensions of the heteroarm star copolymers with respect to the growing second generation of arms (B). Previous results have shown that in some cases the hydrodynamic dimensions of A_nB_n remain the same with those of A_n, although a new set of arms have been growing from the core [7]. On the other hand, in other systems A_nB_n shows significant augmentation of its hydrodynamic dimensions upon the addition of the B arms [6].

In order to elucidate the factors which affect the overall dimensions of the heteroarm star copolymer in solution, a number of series of A_nB_n star copolymer were synthesized. In each series, the number, the length and the nature of the A arms were kept constant while the length and/or the nature of the B arms is varied. In Fig. 2 a number of chromatograms corresponding to a series of PS_nPEMA_n star copolymers together with the PS_n star precursor and the PS (linear) arms are presented.

As it is seen together with the main peak of the A_nB_n star copolymer a small peak exists which coincides with the peak corresponding to the PS linear precursor (arms). This linear residual arises from accidental deactivation during the formation of the PS_n star at the second step of the synthetic procedure. The presence of these residues can be ignored in our analysis and this is one of the benefits of the present method. Our attention focuses on the behavior of the V_R (on peak) of the A_nB_n stars.

Two ways could be applied to evaluate the chromatographic data of Fig. 2. Firstly, we use the difference ΔV_R which according to Eq. (7) expresses the normalized hydrodynamic volume of the A_nB_n star with respect to that of the A_n precursor. In Fig. 3(a) ΔV_R is plotted as a function of the PEMA weight percentage for three the series of PS_nPEMA_n differing on the number of arms.

Secondly the overall dimensions of the star copolymers can be evaluated by converting the primary calibration curve obtained with the PS linear standards

$$\log M = 11,12 - 0,284V_R \quad (8)$$

to a universal type calibration curve in terms of the hydrodynamic radius R_H (nm) by using the scaling relationship valid for the PS/THF system [16]

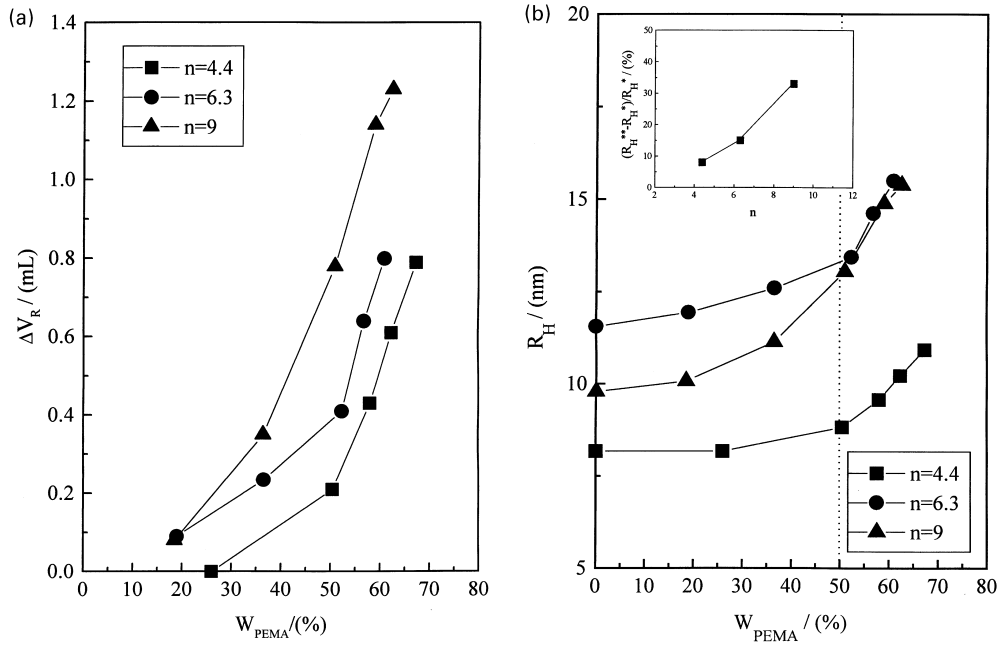

Fig. 3. (a) Variation of ΔV_R versus W_{PEMA} and (b) R_H versus W_{PEMA}, for the three PS_nPEMA_n copolymers series. The inset shows the percentage increase of R_H as a function of the star functionality n, when the molecular weight of the PS_nPEMA_n copolymers is double with respect to PS_n ($W_{PEMA} = 50\%$).

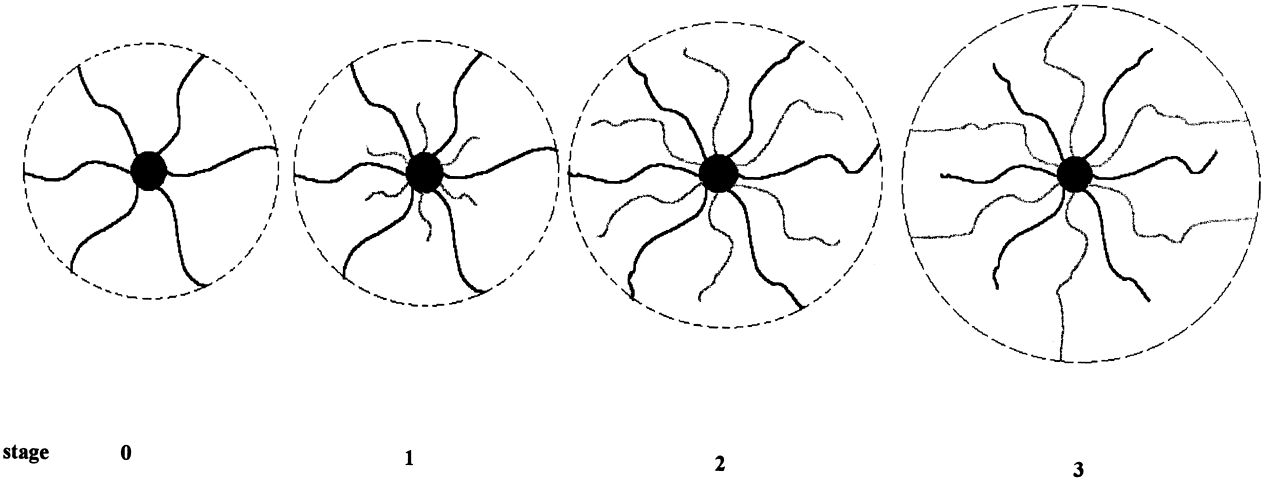

Fig. 4. Schematic representation of the size increase of A_nB_n copolymers as the second set of arms are growing from the core.

$$R_H = (1.37 \times 10^{-2})M^{0.564} \quad (9)$$

therefore Eq. (8) becomes

$$\log R_H = 4.408 - 0.16V_R. \quad (10)$$

In Fig. 3(b) the overall dimensions in terms of hydrodynamic radius, obtained by using Eq. (10) for the three series of PS_nPEMA_n star copolymers differing on the number of arms, have been plotted as a function of the PEMA weight percentage. In fact, Fig. 3(a) and (b) demonstrates the evolution of the hydrodynamic dimensions of a PS_n star macromolecule as a new set of PEMA branches are growing from its core leading to PS_nPEMA_n. As it can be observed different V_h growth rates occur depending on the star functionality n. Several different stages can be distinguished which are presented schematically in Fig. 4. In stage 0 the hydrodynamic size of the star polymer is determined from the number of the PS arms and the length of each arm. In stage 1, where the length of the PEMA arms are still short the overall dimensions remain unaltered. For the PS_n with $n = 4.4$ stage 1 is extended up to 25% W_{PEMA} while for the other samples with higher functionality this stage is shifted to lower W_{PEMA}. At stage 2, where the lengths of the different arms become comparable, there is a smooth increase of the hydrodynamic dimensions depending on the arms number. In the inset of Fig. 3(b) the percentage increase of R_H, where the molecular weight of the heteroarm star copolymer A_nB_n is double with respect to A_n it originates from ($W_{PEMA} = 50\%$), is plotted as a function of the star functionality n. As shown for $n = 4.4$ the R_H value increases by only 8% while for $n = 9$ the increase is 33%. Obviously the dimensions of the heteroarm star copolymer are affected significantly by the number of arms.

Finally in stage 3 the length of the second generation of arms (PEMA) has exceeded that of the first generation of arms (PS) and the dimensions of A_nB_n increase now more sharply. In this case the size of the star-shaped macromolecule is determined mainly by the length of the second set of arms.

In an attempt to understand better how the hydrodynamic volume of the heteroarm star A_nB_n is influenced by the presence of the different arms, we have plotted ΔV_R against the dimensionless ratio L defined as follows:

$$L = \frac{(r^2)_B^{1/2}}{(r^2)_A^{1/2}} \quad (11)$$

where $(r^2)^{1/2}$ is the end-to-end distance expressing the effective size of the arms in the solution [17]

$$(r^2)^{1/2} = \Phi^{-1/3}\{[\eta]M\}^{1/3} \quad (12)$$

where Φ is a constant, $[\eta]$ is the intrinsic viscosity and M the molar mass.

Rearranging $[\eta]$ from the Mark–Houwink–Sakurada equation, $[\eta] = KM^a$, L can be rewritten as

$$L = \left(\frac{K_B M_B^{a_B+1}}{K_A M_A^{a_A+1}}\right)^{1/3}. \quad (13)$$

The constant Φ of Eq. (12) is affected from the number of arms and the solvent quality. Since we use a common good solvent and the number of the different arms are equal the ratio Φ_A/Φ_B is close to unity and has been removed from Eq.

Table 4
Mark–Houwink–Sakurada (MHS) equation's constants

System	K ($\times 10^3$)	a	$\Delta\alpha$ [a]
PS/THF	16 [b]	0.706 [b]	
PEMA/THF	6.04 [c]	0.750 [c]	0.044
PtBA/THF	3.3 [d]	0.800 [d]	0.094
P2VP/THF	14.9 [e]	0.660 [e]	0.046

[a] $\Delta\alpha = |\alpha_{PS} - \alpha_B|$.
[b] From Ref. [22].
[c] From viscosity measurements, this work.
[d] From Ref. [23].
[e] From Ref. [24].

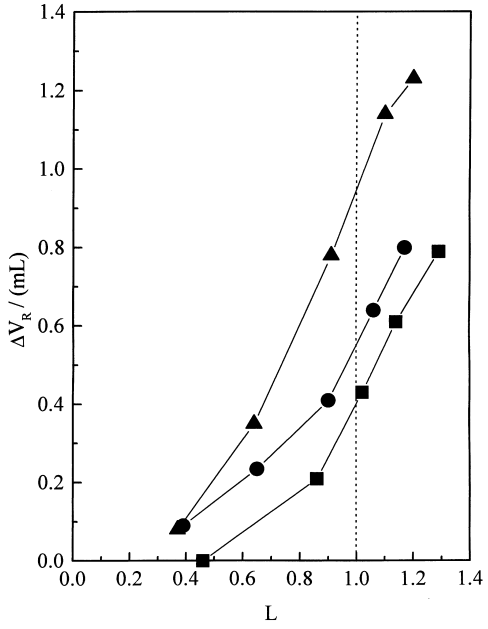

Fig. 5. Plot of ΔV_R as a function of ratio L for the three PS_nPEMA_n copolymers series.

(13). L values were calculated using arm molecular weights from Tables 1–3 and MHS constants from Table 4.

Fig. 5 demonstrates the variation of ΔV_R versus L for the three PS_nPEMA_n star copolymers series. For the sample with the lowest n the hydrodynamic volume of PS_nPEMA_n remains the same with respect to that of PS_n it originates

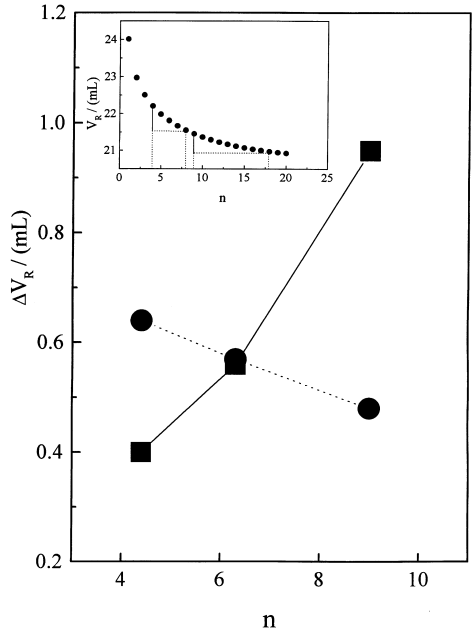

Fig. 6. Star functionality n dependence of ΔV_R passing from PS_n to PS_{2n} (●) and from PS_n to PS_nPEMA_n (■). The inset shows the star functionality n dependence of V_R for PS_n with $M_{br} = 20\,000$, calculated by the Eqs. (8) and (14). The solid lines, in the inset, express the ΔV_R passing from PS_4 to PS_8 and from PS_9 to PS_{18}.

Table 5
Calculated and experimental values of V_R and ΔV_R for PS_n, PS_{2n} and PS_nPEMA_n ($W_{PEMA} = 50\%$) samples

Sample	V_R (ml)		ΔV_R (ml)	
	Calculated[a]	Experimental[b]	Calculated[a]	Experimental[c]
PS_4	21.69	21.85		
PS_8	21.05		0.64	
PS_4PEMA_4				0.4
PS_6	20.93	20.91		
PS_{12}	20.36		0.57	
PS_6PEMA_6				0.56
PS_9	21.43	21.36		
PS_{18}	20.95		0.48	
PS_9PEMA_9				0.95

[a] From Eqs. (8) and (14).
[b] From SEC.
[c] From interpolation to Fig. 5.

from until the effective length of the PEMA arms reaches about 45% of that of the PS arm (stage 1, Fig. 4). Accordingly the hydrodynamic volume increases smoothly until the PEMA arms reach 85% of the PS arm length (stage 2) and finally the V_h of A_nB_n increases further with a higher rate (stage 3).

The hydrodynamic volume for the star polymers with higher number of arms increases more rapidly due to the fact that the segment density increases making the repulsive interactions between the unlike segments of the different arms more effective. This can be demonstrated by plotting ΔV_R at $L = 1$ (where the effective length of the different arms becomes equal) as a function of the star functionality n (Fig. 6).

In the same plot the V_R difference between the PS_n and another star polymer having double number of arms (PS_{2n}) of the same arm length is also shown. The V_R of the PS_{2n} has been calculated by using the equation

$$M_s = M_{br} \cdot n \left[\frac{3n-2}{n^2} \right]^{\varepsilon/\alpha+1} \left[\frac{1-0.276-0.015(n-1)}{1-0.276} \right]^{1/\alpha+1} \quad (14)$$

where M_s is the molecular weight of a linear polymer standard which is eluted at the same retention volume with a star-shaped polymer homolog, having n number of arms of M_{br} molecular weight, a is the MHS exponent of the polymer (standard) solvent system under analysis and ε the exponent of the equation $g = g^{\varepsilon}$ (where g', g are the branching factors) [18]. Therefore V_R can be calculated by using the conventional calibration curve established by linear PS standards (Eq. (8)). The V_R data are collected in Table 5. We see that the calculated values are in excellent agreement with the experimental ones, confirming the validity of Eq. (14).

As shown in Fig. 6 the variation of the dimensions of a homoarm star from PS_n to PS_{2n} decreases with the star functionality. This is expected since V_R of a star-shaped polymer

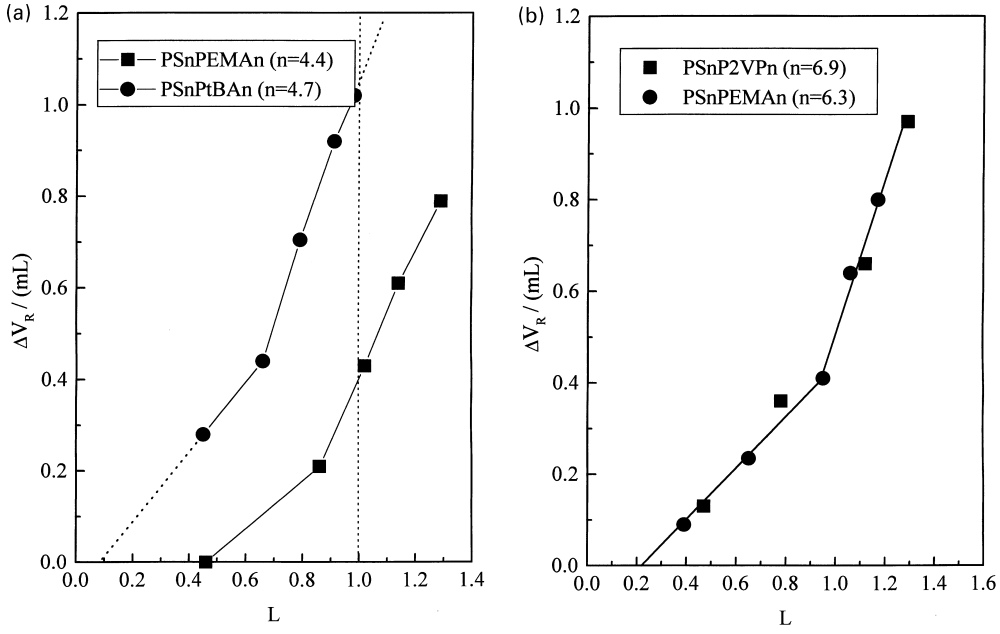

Fig. 7. Plot of ΔV_R as a function of ratio L for (a) PS_nPEMA_n, PS_nPtBA_n and (b) PS_nPEMA_n, PS_nP2VP_n.

decreases exponentially with the star functionality as shown in the inset of Fig. 6. On the contrary, ΔV_R increases in the case of the heteroarm stars passing from PS_n to PS_nPEMA_n due to an increase of the heterocontacts between the different arms and therefore provoking a more stretched conformation of the arms. We observe also that for higher n the hydrodynamic volume of PS_nPEMA_n is higher to that of PS_{2n}, whereas the opposite occurs for the lower n. The two curves are crossing each other at n close to 6, indicating that the excess volume due to the repulsive interactions between the different arms of the heteroarm star becomes positive beyond a certain number of arms. These results also demonstrate, that in some cases the repulsive interactions may lead to a contraction of the one set of arms (PEMA). This occurs for low n where enough space around the star core still exists. Therefore, in this case the hydrodynamic volume of PS_nPEMA_n is lower than that of the PS_{2n}.

By using normalized quantities such as ΔV_R and L we could compare different A_nB_n systems in order to look at the influence of the interactions between the A and B arms. Since we have shown that the functionality of the stars affects remarkably the hydrodynamic dimensions of the macromolecule we have kept n approximately constant. In Fig. 7 the behavior of PS_nPEMA_n is compared with that of PS_nPtBA_n (Fig. 7(a)) and/or with that of PS_nP2VP_n (Fig. 7(b)). In the former case two dinstict curves have been obtained belonging to the different systems whereas in the latter case all the points lay in the same curve.

Table 6
Polymer–polymer interaction parameters for PS with various polymers B

Polymer B	δ_{PS} (cal cm^{-3})$^{1/2}$	δ_B (cal cm^{-3})$^{1/2}$	χ_{PS-B}
PEMA	9.25[a]	8.85[a]	0.027
PtBA	9.25[a]	8.00[a]	0.264
P2VP	9.56[b]	10.4[b]	0.119

[a] According to Hoy tables.
[b] According to Van Krevelen tables.

In order to explain qualitatively the above results the Flory–Huggins interaction parameters χ_{AB} were calculated by using the formula

$$\chi_{AB} = (\delta_A - \delta_B)^2 V_r/RT \quad (15)$$

Where δ_A and δ_B are the Hildebrand solubility parameters for the A and B arms respectively, V_r is the reference volume usually taken to be 100 cm^3/mol and R the gas constant. The solubility parameter of polymers can be estimated from the structural formula using the molar attraction constants F_i and their densities [19] (Table 6).

To explain the differences in behavior between the systems in Fig. 7, the presence of the solvent must be taken into account. As has been shown recently the repulsive interactions between the different polymers are influenced strongly from the selectivity of the solvent which can be expressed by the difference of the MHS exponents $\Delta\alpha$ (see Table 4) [20,21]. Therefore the two factors that govern the hydrodynamic volume of the A_nB_n copolymers are $\Delta\alpha$ and χ_{AB}. For PS_nPtBA_n, the estimated χ_{AB} value is one order of magnitude higher than that of PS_nPEMA_n implying strong incompatibility between the different arms for the former case. The above is further corroborated by a stronger solvent selectivity since $\Delta\alpha = 0.09$. As Fig. 7(a) demonstrates this implies much higher hydrodynamic volumes for PS_nPtBA_n compared to those for PS_nPEMA_n. We also observe that the abrupt variation of the hydrodynamic volume of the

heteroarm star for the former system (stage 3) starts at lower L values with respect to the latter one. Furthermore, stage 1, which is extended up to $L = 0.45$ for PS_nPEMA_n, has been shifted now to $L = 0.1$ for the PS_nPtBA_n. Finally the ΔV_R for $L = 1$ is about 1.1 ml for PS_nPtBA_n which is even higher than the corresponding PS_{2n} (Fig. 6) demonstrating that the strong repulsive interactions even for low star functionality ($n = 4.7$) provoke significant variation of the dimensions of the heteroarm star copolymer compared to those of the PS_{2n}.

It is interest to compare the systems PS_nP2VP_n and PS_nPEMA_n. In this case their hydrodynamic behavior coincide (common curve in Fig. 7(b)) although χ_{AB} are different. The above results could be attributed to the fact that $\Delta\alpha$ for both systems are identical and of low magnitude (0.045). As reported by Dondos et al. for the system PS/PMMA/$CHCl_3$ when $\Delta\alpha$ becomes 0.05 at 50°C the repulsive interactions are suppressed and compatibily between the two polymers is favored [20]. This resembles our system that exhibits the same level of selectivity. In conclusion we may say that in the case where χ_{AB} does not differ very much the key factor affecting the hydrodynamic behavior of the copolymer is the selectivity of the solvent.

4. Conclusions

Size exclusion chromatography was used to characterize the hydrodynamic behavior of the heteroarm star copolymers A_nB_n in a common good solvent. The proposed method allows the study of the evolution of the hydrodynamic dimensions of the heteroarm star copolymers as the second generation of the arms is growing from the cores. By monitoring the difference ΔV_R between the retention volumes of the A_nB_n and A_n precursor (which is proportional to the normalized hydrodynamic volume of A_nB_n) as a function of the dimensionless ratio L of the effective size of the different arm lengths, interesting conclusions have been drawn. The dimensions of A_nB_n are growing passing several stages depending on the ratio of the effective size of the different arms. In an early stage the size of the heteroarm stars remain stable until a certain length of the second generation of arms is reached. In an intermediate state the A_nB_n dimensions increase smoothly until the length of the B arms become comparable with that of the A arms. Finally in a prolonged stage the star size increases in a higher rate since the length of the B arms exceed that of the A arms. The star functionality and the interaction of the unlike segments between the different arms influence remarkably the different stages of the heteroarm star size growth. As the functionality and/or the incompatibility of the different arms increases, these stages occur at lower A,B arm length ratios, L. In other words at a given L the higher the star functionality and/or A,B incompatibility the higher the hydrodynamic volume of the A_nB_n star polymer.

References

[1] Tsitsilianis C, Chaumont P, Remp P. Makromol Chem 1990;191:2319.
[2] Quirk RP, Lee B. Polym Prepr, Am Chem Soc Div Polym Chem 1991;32:607.
[3] Kanaoka S, Omura T, Sawamoto M, Higashimura T. Macromolecules 1992;25:6497.
[4] Iatrou K, Hadjichristidis N. Macromolecules 1992;25:4649.
[5] Ishizu K, Kuwahara K. J Polym Sci, Part A: Polym Chem 1993;31:661.
[6] Tsitsilianis C, Graff S, Rempp P. Eur Polym J 1991;27:243.
[7] Tsitsilianis C, Papanagopoulos D, Lutz P. Polymer 1995;36:7345.
[8] Tsitsilianis C, Voulgaris D. Macromol Chem Phys 1997;198:997.
[9] Tsitsilianis C, Kouli O. Makromol Rapid Commun 1995;16:591.
[10] Vlahos CH, Horta A, Hadjichristidis N, Freire JJ. Macromolecules 1995;28:1500.
[11] Iatrou H, Siakali Kioulafa E, Hadjichristidis N, Roovers J, Mays J. J Polym Sci, Part B: Polym Phys 1993;33:19–25.
[12] Vlahos C, Tselikas Y, Hadjichristidis N, Roovers J, Rey A, Freire J. Macromolecules 1996;29:5599.
[13] Voulgaris D, Tsitsilianis C, Esselink FJ, Hatziioannou G. Polymer 1998;39:6429.
[14] Pispas S, Poulos Y, Hadjichristidis N. Macromolecules 1998;31:4181.
[15] Voulgaris D, Tsitsilianis C, Grayer V, Esselink FG, Hadziioannou E. Polymer 1999, in press.
[16] Mandema W, Zeldenrust H. Polymer 1997;18:835.
[17] Flory PJ. Principles of polymer chemistry. Ithaca, NY: Cornell University Press, 1953.
[18] Tsitsilianis C, Ktoridis A. Macromol Rapid Commun 1994;15:845.
[19] Van Krerelen DW. Properties of polymers, 2nd ed. Amsterdam: Elsevier, 1976.
[20] Christopoulou V, Papanagopoulos D, Dondos A. J Polym Sci, Part B: Polym Phys 1998;36:1051.
[21] Dondos A, Christopoulou V, Papanagopoulos D. J Polym Sci, Part B: Polym Phys 1999;37:379.
[22] Alliet DF, Pacco JM. Sixth GPC Seminar, Miami, FL, October 1968.
[23] Mrkvickova L, Danhelka J. J Appl Polym Sci 1990;41:1929.
[24] Mencer HJ, Crubisic Z, Gallot Y. J Liquid Chromatography 1979;2(5):649.